Available online at www.sciencedirect.com

ScienceDirect

Scripta Materialia 103 (2015) 65–68

Scripta MATERIALIA

www.elsevier.com/locate/scriptamat

The role of free surfaces on the formation of prismatic dislocation loops

Lynn B. Munday,* Joshua C. Crone and Jaroslaw Knap

RDRL-CIH-C, U.S. Army Research Laboratory, Aberdeen Proving Ground, MD 21005, USA

Received 27 January 2015; revised 3 March 2015; accepted 3 March 2015
Available online 28 March 2015

Prismatic punching is a process where voids grow through the nucleation and emission of prismatic dislocation loops (PDLs). In this work we employ dislocation dynamics to determine the effect of image stresses produced by the void's free surface on PDL formation in a face-centered cubic lattice. We find that image stresses cause PDL formation to fall into two distinct pressure regimes. In the low pressure regime, image stresses dominate dislocation cross-slip, reducing the PDL's size and formation rate.
Published by Elsevier Ltd. on behalf of Acta Materialia Inc.

Keywords: Dislocation dynamics; Void growth; Image stress; Cross-slip

During the initial stages of void growth, dislocations nucleated from the void's surface are assumed to punch out material from the void [1]. However, dislocations nucleated as glide loops with a Burgers vector in the plane of the loop cannot remove material. It is only after the conversion of the glide loop into a prismatic dislocation loop (PDL) with a Burgers vector normal to the loop that material removal through punching is possible [2]. The conversion from a nucleated dislocation into a PDL can occur through an interaction with dislocations on other glide planes or through multiple cross-slip events [3,4]. In both formation mechanisms, the PDL is assumed to form under the action of the stress concentrators arising from the far-field load's interaction with the void. In this letter we report a new limiting factor on PDL formation. We show that image stresses produced by the interaction of the dislocation with the void's free surface dominate PDL formation for pressures below 3.0 GPa and limit void growth.

Plastic void growth occurs during the ductile failure process where high-strain loading leads to void nucleation, growth, and coalescence into microcracks. After a nano-sized void is nucleated at a weak spot in the lattice, it grows plastically through dislocation related processes. The initial stages of void growth occurs through the nucleation of dislocations from the void's surface [3,5]. Dislocation nucleation remains active up to micron sized voids at which point the density of dislocations in the material becomes large enough to support continued plastic growth through dislocation multiplication [6]. At the early stages, submicron void growth becomes strongly dependent on the discrete volume changes due to the formation and emission of individual PDLs.

High strain rates and small void sizes, typical for atomistic simulations, reveal PDL formation via interaction of multiple nucleated dislocation loops on different glide planes [3]. In a stark contrast to the high-strain rate simulations, Ashby and Johnson [4] describe a fully 3D mechanism for PDL formation around a spherical particle as originating from a single incipient dislocation loop. In their model, the misfit particle induces a stress field equivalent to that of a void under far-field hydrostatic stress [7]. Under the action of this stress field, the incipient dislocation loop expands out from the particle, cross-slipping onto other glide planes once it becomes energetically favourable. After a sequence of four cross-slip events, a PDL is finally formed.

Ashby and Johnson's model was developed for PDL formation around a particle and therefore does not include the effect of the void's free surface on dislocation cross-slip. However, image forces arising from the dislocation's interaction with the free surface have been shown to be influential on cross-slip in previous atomistic and dislocation dynamics simulations [8,9]. In this work, we employ 3D dislocation dynamics to determine the effects of these image stresses on the mechanisms which allow an incipient dislocation loop nucleated from the surface of a void to evolve into a PDL. Our simulations are based on the dislocation dynamics formulation of van der Giessen and Needleman [10]. In this formulation, the stress fields due to dislocations in an infinite perfect crystal are combined with those obtained from a solution of an auxiliary boundary value problem with suitable traction boundary conditions. We utilize the Parallel Dislocation Simulator (ParaDiS) [11] for the former and a parallel finite element code for the latter [12,13].

* Corresponding author; e-mail: lynn.b.munday.civ@mail.mil

http://dx.doi.org/10.1016/j.scriptamat.2015.03.009
1359-6462/Published by Elsevier Ltd. on behalf of Acta Materialia Inc.

The material considered is a model face-centered cubic (fcc) crystal of aluminum with shear modulus $\mu = 27$ GPa, Poisson's ratio $\nu = 0.35$ and Burgers vector magnitude $|\mathbf{b}| = 2.86$ Å. A linear mobility function is employed to relate the force on the dislocation to its velocity through $f_i = B_i v_i$. Here, f is the dislocation force, B is the drag coefficient, v is the dislocation velocity and subscript i indicates the dislocation character, either edge or screw. We assume that drag coefficients in the linear mobility function satisfy $B_{screw}/B_{edge} = 2$. The above ratio has been determined by Olmsted et al. [14] from atomistic simulations. We emphasize that according to this mobility function, the same stress value will propel edge dislocations to move twice as fast as screw dislocations. Thus, screw oriented dislocations able to cross-slip will be preferred. Moreover, since only dislocations with a full Burgers vector are modeled, cross-slip of screw dislocations will occur once stresses become favourable. Finally, we emphasize that the local force on the dislocation includes Peach–Koehler forces from other dislocations and the far-field loading as well as the dislocation's self-energy by recourse to the line-tension model.

Our computational domain is a cube of edge length $l = 25{,}000\ |\mathbf{b}|$ containing a single void of radius $R_v = 100\ |\mathbf{b}|$ at the center. Tractions imposing a uniform stress field $\boldsymbol{\sigma}^\infty = p\mathbf{I}$, where $\mathbf{I}$ is the identity tensor and $p > 0$, are applied to the outer cube boundaries. It bears emphasis that pressure p is being defined as hydrostatic tension. Image tractions due to the dislocations are applied to the void surface. We discretize the computational domain with variable sized quadratic tetrahedral elements yielding a 2.5 $|\mathbf{b}|$ resolution in the vicinity of the void.

Dislocation nucleation is not examined in the present work and all dislocations are assumed to originate from an incipient dislocation structure. The nucleation of any incipient dislocation structure around the void is driven by the resolved shear stress on a glide plane defined as $\sigma_{bn} = \hat{\mathbf{n}} \cdot \boldsymbol{\sigma} \cdot \hat{\mathbf{b}}$, where $\boldsymbol{\sigma}, \hat{\mathbf{b}} = \mathbf{b}/|\mathbf{b}|$, $\hat{\mathbf{n}} = \mathbf{n}/|\mathbf{n}|$ are the stress, the unit Burgers vector and the unit normal of the glide plane, respectively. In Figure 1, we plot σ_{bn} in the region near the void for the two families of glide planes: (a) $\mathbf{n} = (1\,1\,1)$ and (b) $\mathbf{n} = (\bar{1}\,\bar{1}\,1)$ sharing the Burgers vector $\mathbf{b} = [\bar{1}\,1\,0]$. An ideal PDL with $\mathbf{b} = [\bar{1}\,1\,0]$ shown by the blue and red lines in Figure 1(c) is made up of a continuous dislocation loop gliding on these families of glide planes denoted by the dashed lines and numbered (*i*) through (*iv*). The Burgers vector $\mathbf{b} = [\bar{1}\,1\,0]$ of this PDL is oriented toward the reader. Under the action of $\boldsymbol{\sigma}^\infty$, the maximum of $\sigma_{bn} = \pm\frac{3}{4}p$ for each of the two glide planes is located at a distance of $R_v/\sqrt{2}$ from the center. In order to mimic the effect of dislocation nucleation in our simulations, an incipient dislocation configuration composed of a $[\bar{1}\,1\,0](1\,1\,1)$-type dislocation glide loop with radius $R_L = 25\ |\mathbf{b}|$ is placed on the void surface at the position of the maximum resolved shear stress, as indicated in Figure 1(c). We emphasize that this incipient dislocation loop is not always stable as it is drawn into the void if $p \leqslant 1.4$ GPa.

We start by assessing the sequence of events assumed by Ashby and Johnson's classical model for PDL formation. In order to account for free surfaces in our simulations, dislocations intersecting the surface are terminated with the end on the surface constrained to move along the surface. Moreover, we approximate free surface effects on the dislocation self energy by removing line-tension forces at the surface. We connect dislocation surface nodes via so-called virtual dislocations to the center of the void as to maintain a zero net Burgers vector for the surface terminated dislocations [15]. We point out that the above

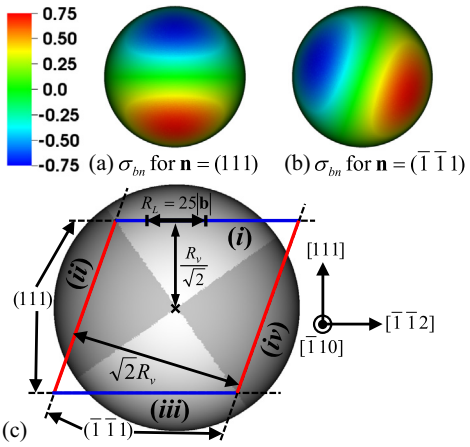

Figure 1. Glide stress due to the far-field load near the void surface for $\mathbf{b} = [\bar{1}\,1\,0]$ and glide plane normals (a) $\mathbf{n} = (1\,1\,1)$ or (b) $\mathbf{n} = (\bar{1}\,\bar{1}\,1)$. The colourbar shows the normalized stress, σ_{bn}/p. (c) Void surface coloured by the glide plane maximizing σ_{bn}. The light grey quadrant indicates the region where $|\sigma_{b\mathbf{n}=(1\,1\,1)}| > |\sigma_{b\mathbf{n}=(\bar{1}\,\bar{1}\,1)}|$ and dark grey indicates the opposite. Light grey quadrants favour growth of $[\bar{1}\,1\,0](1\,1\,1)$ type dislocations shown in blue and dark grey quadrants favour growth of $[\bar{1}\,1\,0](\bar{1}\,\bar{1}\,1)$ type dislocations shown in red. The incipient $[\bar{1}\,1\,0](1\,1\,1)$ dislocation loop is dimensioned and labeled R_L. The red and blue lines indicate the ideal PDL that would be generated from the incipient dislocation and passes through points maximizing σ_{bn}. Each glide plane of the PDL is labeled (*i*–*iv*). (For interpretation of the references to colour in this figure legend, the reader is referred to the web version of this article.)

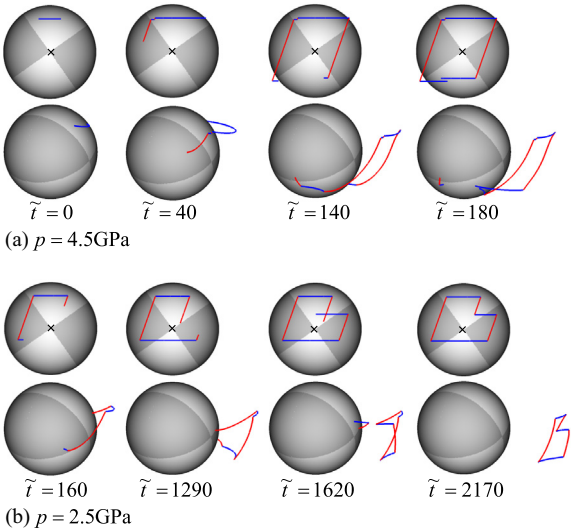

Figure 2. Evolution of an incipient dislocation loop into a PDL for (a) $p = 4.5$ GPa and (b) $p = 2.5$ GPa. Two views of the PDL are shown at each time step labeled by $\tilde{t}$ with units GPa^{-1}. The top view showing the contour of the PDL uses the coordinate system in Figure 1. The lower view shows the profile of the PDL peeling off in the $\mathbf{b} = [\bar{1}\,1\,0]$ direction. Dislocation and void quadrant colouring are described in Figure 1(c).